Journal of Urban and Environmental Engineering, v.7, n.1, p.151-156

ISSN 1982-3932
doi: 10.4090/juee.2013.v7n1.151156

Journal of Urban and Environmental Engineering

www.journal-uee.org

FLOW PHYSICS OF 3-BLADED STRAIGHT CHORD H-DARRIEUS WIND TURBINE

Rajat Gupta[1] and Agnimitra Biswas[2*]

[1]Director, National Institute of Technology Srinagar, Srinagar, Jammu & Kashmir, India

[2]Assistent Professor, National Institute of Technology Silchar, Silchar, Assam, India

Received 30 March 2013; received in revised form 9 May 2013; accepted 30 May 2013

Abstract: Steady-state two-dimensional Computational Fluid Dynamics (CFD) simulations were performed using Fluent 6.0 software to analyze the flow physics of 3-bladed straight chord H-Darrieus wind turbine having blade twist of 300 for 10% of its chord at the trailing ends. The flow was simulated using finite volume method coupled with moving mesh technique to solve mass and momentum conservation equations. The standard k-ε turbulence model with enhanced wall condition was used. Second-order upwind discretization scheme was adopted for pressure-velocity coupling of the flow. Flow physics of the turbine was analyzed with the help of pressure and velocity contours. It was found that velocity magnitude decreases from upstream to downstream side across the turbine, which will cause overall lift for the turbine. Further, blade twist at the trailing ends creates circulations that interact with the blades in a direction opposite to the direction of rotation of the turbine which would enhance power production for the three bladed turbine.

Keywords: H-Darrieus turbine, straight chord blade, CFD analysis, contours

[*] Correspondence to: Agnimitra Biswas, Tel.: Fax: +091-3842-233797, Phone: +0091-3842-248308.
E-mail: agnibis@yahoo.co.in

INTRODUCTION

The straight-bladed Vertical Axis Wind Turbine (VAWT), H-Darrieus turbine, is an invention included in the Darrieus patent (Darrieus, 1931). The H-Darrieus turbine, also known as H-rotor after its inventor, is a lift type device, which has two to three blades designed as airfoils. The blades are attached vertically to the central shaft through support arms. The support to the vertical axis helps the turbine maintain its shape. The H-Darrieus turbine is normally placed on the top of a tower in order to reach higher winds. Moreover, the H-Darrieus turbine is the most suitable turbine in extreme wind conditions, like wind gusts, cyclone, and its efficiency could be as high as Horizontal Axis Wind Turbine (HAWT) when placed on rooftops (Mertens, 2003).

Guy wires are generally used to support the shaft of eggbeater Darrieus turbine since it gives a stiffer, more robust construction. However, guy wires are optional for H-Darrieus turbine, which is an advantage. It is self-regulating in all wind speeds reaching its optimal rotational speed shortly after its cut-in wind speed (Islam *et al.*, 2005). The blades of H-Darrieus turbine are much easier to manufacture than the blades of a HAWT or of an eggbeater Darrieus turbine. Light weight, highly flexible turbines are usually two-bladed turbines. Visual aesthetics and lower noise are the reasons for using three-bladed designs. Tangtonsakulwong & Chitsomboon (2006) did Computational Fluid Dynamics (CFD) simulation of wind flow over an untwisted three-bladed H-Darrieus turbine of NACA 0015 blade profile by using 3D unstructured-mesh finite volume method together with the sliding mesh technique to solve mass and momentum conservation equations. The maximum power coefficient of 0.20 was obtained at a tip speed ratio of 2.9. Jiang et al. (2007) developed 2D CFD models to study the effects of number of blades and tip speed ratio on the performance of multi-bladed H-Darrieus turbines. However, the highest power coefficient of their turbine was about 19%. Howell et al. (2010) studied the performances of two-bladed and three-bladed H-Darrieus turbines through wind tunnel experiments and also through CFD analyses. The two-bladed turbine had a higher peak power coefficient of 0.25 compared to about 0.22 for the three-bladed turbine.

Twist blades could be a good field of research since such blades have the potential to be superior to the untwisted blades. Tip geometry can locally modify the angle of attack and the inflow dynamic pressure and hence can improve performance of the turbine. But experimental or computational works in this direction are very few. Keeping this in view, in this paper, an attempt was made to study the performance of a three-bladed H-Darrieus turbine having blade twist of 30^0 for 10% of its chord at the trailing ends. Two dimensional simulations were run using **Fluent 6.0** CFD software. Pressure and velocity contours were analyzed and performance of the present turbine was predicted from the analysis.

Model Design

The height of the turbine was 20cm, and the chord length of the blades was 5 cm. An angular twist of 30^0 was provided at the tips of the chords for 10% of chord length from the trailing end. The turbine is shown in the **Fig.1** respectively. The blades were supported on bolts 5mm in diameter & 12 cm in length. The central shaft of the turbines was 1.5 cm in diameter and about 25 cm in length. By changing the overall turbine diameter but keeping the height constant, ten numbers of H/D ratios were obtained. The central shaft, base and the supports were made from mild steel, and the blades were made from lightweight aluminium. Ball bearings were used to support the shaft of the turbines at the base. The base was 7cm wide and 2.4 cm thick.

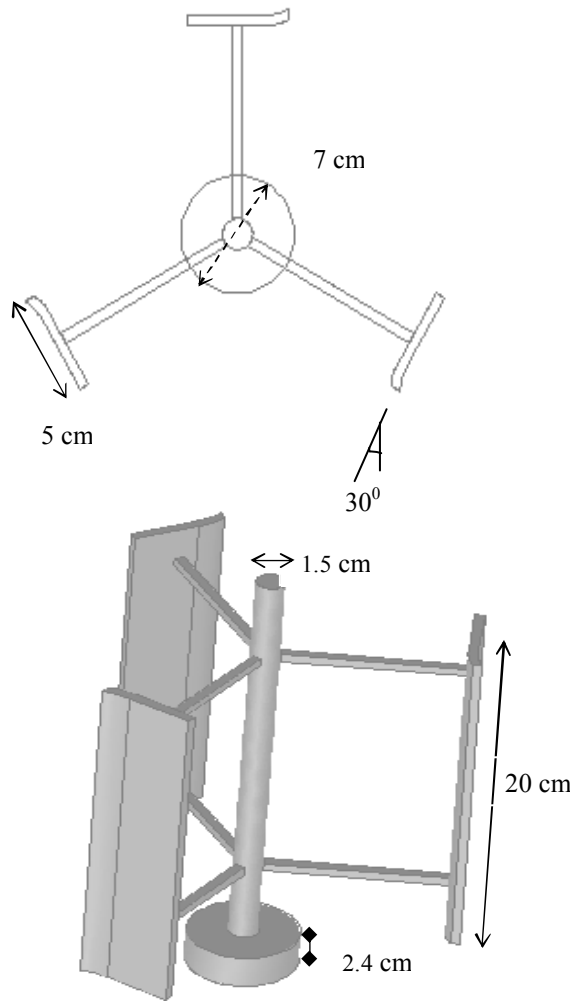

Fig. 1 Three-bladed straight chord H-Darrieus turbine

The Computational Approach

The CFD simulations were carried out using Fluent 6.0 software in which the meshing was done in Gambit. The computational models of the turbine along with the boundary conditions are shown in **Fig. 2**. Velocity inlet and outflow conditions were taken on the left and right boundaries respectively. The top and bottom boundaries of the computational domain, which signify the sidewalls of the wind tunnel, had symmetry conditions on them. The blades, central shaft and the support arms were set to standard wall conditions. On the four surrounding edges of the computational domain, uniform grids were taken. The density of the mesh was higher at the blade ends since sudden change in blade section at the ends requires more dense nodes on them**.** The distance of the first row of grid points (i.e. nodes) in direction normal to the solid boundary was 0.0001 cm. Unstructured (triangular) meshing was done on the face external to the turbines. The computations were initially carried out with various levels of refinement for the mesh until the Grid Independent Limit (GIL) mesh Masson et al. (1997) was attained. Each refinement level was solved in Fluent with the same set of input parameters. The unstructured triangular mesh around an airfoil blade of such turbine is shown in **Fig. 3**.

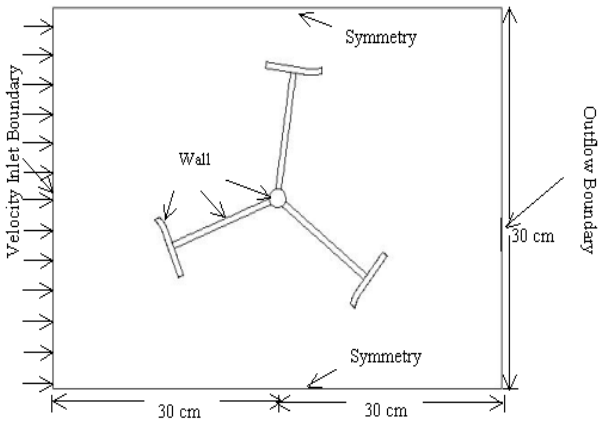

Fig. 2 Computational domain of the 3-bladed straight chord H-Darrieus turbine

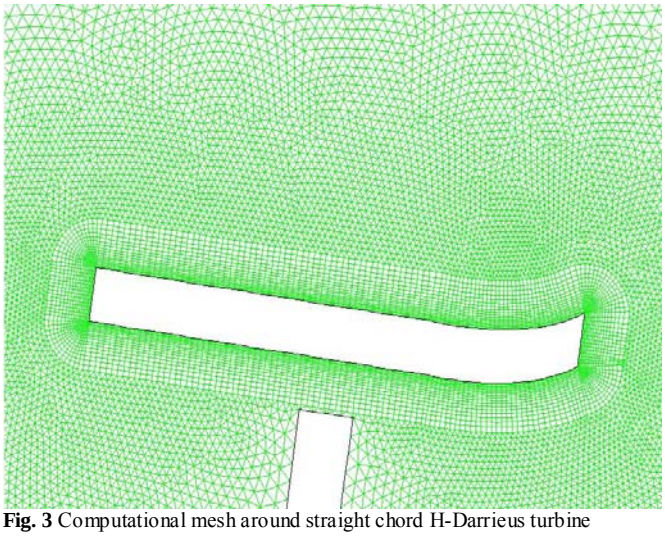

Fig. 3 Computational mesh around straight chord H-Darrieus turbine

CFD Formulation

The Navier-Stokes equation in finite difference form for incompressible flow of constant viscosity is solved by the in-built functions of the fluent CFD package. Similarly, the finite difference forms of continuity and turbulence equations are solved. The simplest and most widely used two-equation turbulence model is the standard k-ε model that solves two separate transport equations to allow the turbulent kinetic energy and its dissipation rate to be independently determined. The

standard k– ε model is particularly suitable for flows though sharp corners, straight and curved edges like the turbine blades as the model uses wall functions based on the law of the wall. The k– ε can be represented as:

$$\frac{\partial}{\partial t}(\rho k)+\frac{\partial}{\partial x_i}(\rho k u_i)=\frac{\partial}{\partial x_j}\left[\left(\mu+\frac{\mu_t}{\sigma_k}\right)\frac{\partial k}{\partial x_j}\right] \quad (1)$$
$$+G_k-\rho\varepsilon-Y_M$$

$$\frac{\partial}{\partial t}(\rho\varepsilon)+\frac{\partial}{\partial x_i}(\rho\varepsilon u_i)=\frac{\partial}{\partial x_j}\left[\left(\mu+\frac{\mu_t}{\sigma_\varepsilon}\right)\frac{\partial \varepsilon}{\partial x_j}\right]+ \quad (2)$$
$$C_{1\varepsilon}\frac{\varepsilon}{k}(G_k)-C_{2\varepsilon}\rho\frac{\varepsilon^2}{k}$$

Equation 1 corresponds to turbulent kinetic energy equation in which the first and second term on the left hand side represent local and convective turbulent kinetic energies per unit mass respectively; first term on the right hand side is the stress tensor for turbulent kinetic energy, 'G_k' meaning generation of turbulence due to viscous forces, 'ρε' meaning turbulence dissipation rate per unit specific volume and 'Y_M' meaning momentum source. Similarly eq^n 2 corresponds to turbulence dissipation rate equation in which left hand side terms correspond to local and convective dissipation rates per unit mass; first term on right hand side is the stress tensor for turbulent dissipation rate and the remaining terms correspond to source terms for dissipation. The values of the five constants of the standard k-ε turbulence model are taken as:

$$C_\mu = 0.09 \quad C_{1\varepsilon}=1.44 \quad C_{2\varepsilon}=1.44 \quad \sigma_k=1.0$$
$$\sigma_\varepsilon=1.3$$

In this study, steady state, incompressible flow was considered. The numerical simulation was carried out by solving the conservation equations for mass and momentum and by using an unstructured-grid finite volume methodology coupled with moving mesh technique (FLUENT, 2005). The standard k-ε turbulence model with enhanced wall function was utilized. The method of dynamic grid or rotating reference frame was implemented in which the blade is fixed in the view of an observer who is moving with the rotating frame of reference. Single rotating reference frame was considered, where the blades along with the support arms and the central shaft rotate relative to the incoming fluid stream. The sequential algorithm, Semi-Implicit Method for Pressure-Linked Equation (SIMPLE), was used for solving all the scalar variables. For the convective terms of the momentum equations and also for the turbulence equations**,** the second order upwind interpolating scheme Versteeg and Malalasekera (1995) was adopted in order to achieve accurate results. The iterations are continued until the residual values had dropped to 1×10^{-3}.

CFD Analysis of 3-bladed Straight Chord H-Darrieus Turbine

The contour plots of pressure and velocity magnitude are analysed. These plots are generated at the tip speed ratios for which the power coefficients of the turbines were the highest. The **Fig. 4** shows static pressure contours at 5^0, 125^0 and 245^0. **Figure 5** shows static pressure contours for blade angles: 90^0, 210^0 and 330^0. The blade angles are to be counted starting from the left, i.e. upstream side and then moving in the clockwise direction. The pressure contour plots show a decrease of static pressure from the upstream side to the downstream side across the turbine. For blade angles of 5^0, 125^0 and 245^0 of the straight chord turbine, i.e. for the advancing blade at 5^0, **Fig. 4** shows that the static pressure decreases from 1.89×10^2 Pascal in the upstream side to 9.63×10^1 Pascal in the downstream side across the turbine. Similarly, **Fig. 5** of the straight chord turbine for blade angles of 90^0, 210^0 and 330^0 shows that static pressure decreases from 6.38×10^2 Pascal in the upstream side to 1.21×10^2 Pascal in the downstream sides. Thus, the amounts by which the static pressures decrease across the turbines increase with the increase of the blade angle of rotation.

The static pressure contours further show that circulations or vortices are generated on the blade ends. These circulations are generated in areas very close to the blade ends, and there is a close interaction of these circulations with the blades as well. Although these interactions are more for the turbine, such effects would simultaneously increase the drag on the three-bladed turbine. Further, the static pressures are negative near the ends of the blades meaning circulations at the blade ends were in a direction opposite to the direction of rotation of the turbine thereby would enhance power production for the three bladed turbine. However, the pressure at the exit of the computational domain is positive that means bulk flow is uniform throughout the computational domain. The dynamic pressure contour of the turbine for blade angles of 90^0, 210^0 and 330^0 is shown in **Fig. 6**. It shows that the dynamic pressure is positive in the computational domain meaning the flow physics are alright. Moreover, it further shows that the dynamic pressures are high and positive on the blade ends where static pressures are negative as the total pressure is constant for any location within the flow domain. Further, it can be observed from that the dynamic pressure is very high (of the order 10^3 Pascal)

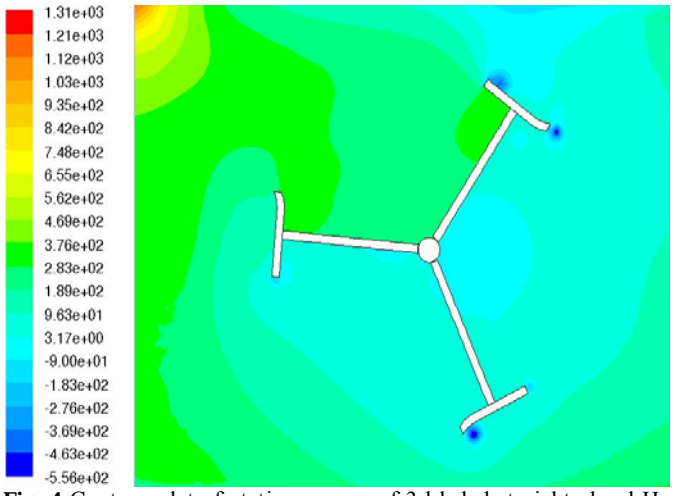

Fig. 4 Contour plot of static pressure of 3-bladed straight chord H-Darrieus turbine having Al blades for blade angle: 5^0, 125^0 and 245^0

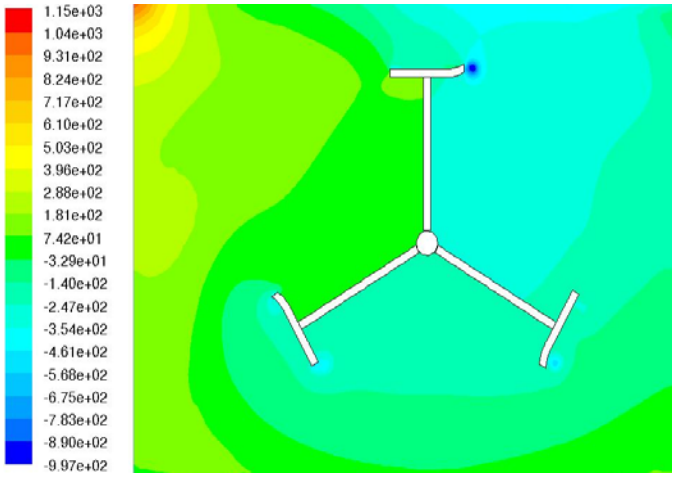

Fig. 5 Contour plot of static pressure of 3-bladed straight chord H-Darrieus turbine having Al blades for blade angle: 90^0, 210^0 and 330^0

for the blades at 330^0 positions (upstream side). This would have been caused due to the twisted shape of the blades. And it would result in the increased performance for the twist bladed turbines especially in the upstream side.

Figure 7 shows velocity contour of the turbine for blade angles of 90^0, 210^0 and 330^0. The blade angles are to be counted starting from the left, i.e. upstream side and then moving in the clockwise direction. The velocity contour shows that there is a decrease of velocity magnitude from the upstream side to the downstream side across the turbine. The difference of velocity magnitude causes overall lift for the turbine. **Figure 7** shows that velocity magnitude decreases from 17.7 m/sec upstream to 8.97 m/sec downstream. Now, for the blade at 330^0 position, the velocity magnitude is very high on the immediate upstream of the blades due to high intensity of dynamic pressure. On the downstream of the blade, the velocity is around 13 m/sec to 15 m/sec.

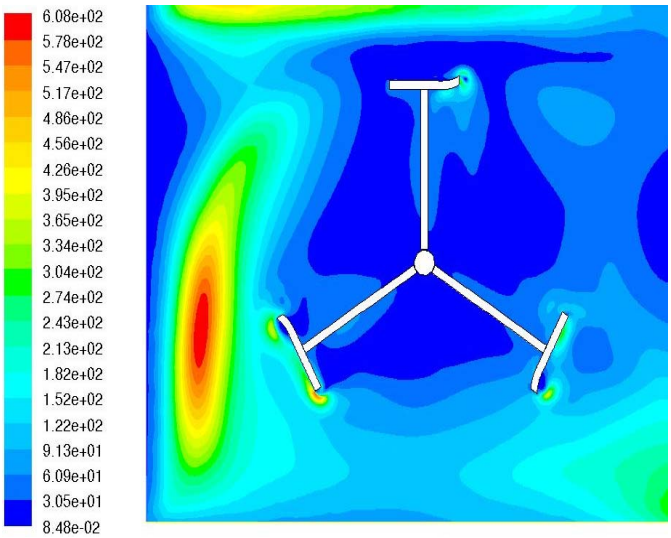

Fig. 6 Contour plot of dynamic pressure of 3-bladed straight chord H-Darrieus turbine for blade angle: 90^0, 210^0 and 330^0

CONCLUSIONS

Steady-state two-dimensional CFD simulations were performed using Fluent 6.0 software to analyze the flow physics of 3-bladed straight chord H-Darrieus wind turbine. From the present study, the following conclusions are summarized:

1. Static pressure decreases from upstream side to downstream side of the rotor. With increase in blade rotation, static pressure drop across the rotor increases thereby propelling the rotor in its power stroke by creating useful pressure difference across the blade. Static pressures are negative near the ends of the blades but the pressure at the exit of the computational domain is positive. Dynamic pressure is positive throughout the computational domain as expected from the flow physics.

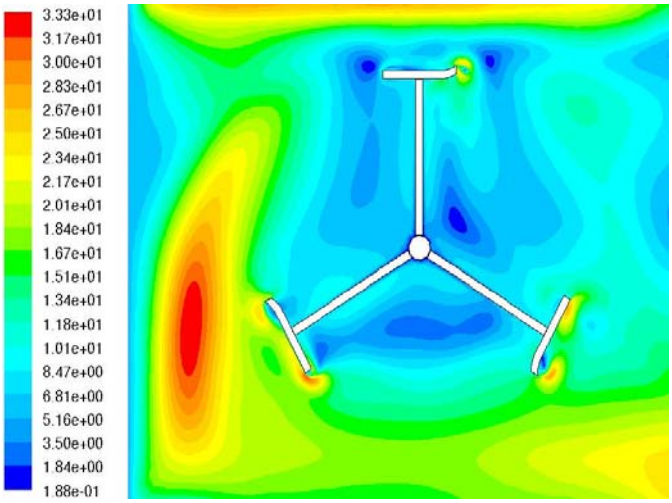

Fig. 7 Contour plot of velocity magnitude of 3-bladed straight chord H-Darrieus turbine having Al blades for blade angle: 90^0, 210^0 and 330^0

2. There is a decrease of velocity magnitude from the upstream side to the downstream side across the turbine as the energy from wind is extracted by the turbine.

3. The blade twist at the trailing ends creates circulations that interact with the blades in a direction opposite to the direction of rotation of the turbine which would enhance power production for the three bladed turbine.

REFERENCES

Darrieus G.J.M (1931). Turbine having its rotating shaft transverse to the flow of the current, US Patent No 1 835 018.

FLUENT Inc. Fluent 6.2 documentation: user's guide. 2005.

Howell, R., Qin, N., Edwards, J., Durrani, N. (2010). Wind tunnel and numerical study of a small vertical axis wind turbine. Renewable Energy Journal, **35**(4), 412-422 .

Islam M., Esfahanian V., Ting D.S-K., Fartaj A (2005). Applications of Vertical Axis Wind Turbines for Remote Areas. In: Proceedings of 5th Iran National Energy Conference, Tehran.

Jiang, Z.-C., Doi, Y., Zhang, S.-Y. (2007). Numerical investigation on the flow and power of small-sized multi-bladed straight Darrieus wind turbine. Journal of Zhejiang Univ Sci A, **8**(9), 1414-1421.

Masson, C., Ammara, I., Paraschivoiu, I. (1997). An aerodynamic method for the analysis of isolated horizontal-axis wind turbines, Int. J. of Rotating Machinery, **3**(1), 21-32.

Mertens S., The energy yield of roof mounted wind turbines, Journal of Wind Engg, **27**(6), 507–518.

Tangtonsakulwong, J., Chitsomboon, T. (2006). Simulation of flow over a 3-blade vertical axis wind turbine. In Proceedings: the 2nd Thailand national energy conference, Thailand, July, 2006.

Versteeg, H.K., Malalasekera, W. (1995). An introduction to computational fluid Dynamics, the finite volume method. In: Longman Scientific & Technical, New York, 132.